Supporting Information

Elucidating the Mechanistic Origins of Photocatalytic Hydrogen Evolution Mediated by MoS_2/CdS Quantum-Dot Heterostructures

Junsang Cho,[a,b]† Nuwanthi S. Suwandaratne,[c]† Sara Razek,[d] Yun-Hyuk Choi,[a,e] Louis F. J. Piper,[d]* David F. Watson,[c]* Sarbajit Banerjee*[a]

[a]Departments of Chemistry and Materials Science and Engineering, Texas A&M University, College Station, TX 77842-3012 (USA)
[b]Department of Chemistry, Duksung Women's University, Seoul 01369, South Korea
[c]Department of Chemistry, University at Buffalo, The State University of New York, Buffalo, NY 14260-3000 (USA)
[d]Department of Physics, Applied Physics and Astronomy, Binghamton University, Binghamton, New York 13902, USA
[e]School of Advanced Materials and Chemical Engineering, Daegu Catholic University, Gyeongsan, Gyeongbuk 38430, South Korea

† These authors contributed equally.

Corresponding Authors: lpiper@binghamton.edu; dwatson3@buffalo.edu; banerjee@chem.tamu.edu

Table of Contents

Figure S1.....S2

Figure S2.....S3

Figure S3.....S4

Figure S4.....S5

Figure S5.....S6

Figure S6.....S7

Tables S1 and S2.....S8

.

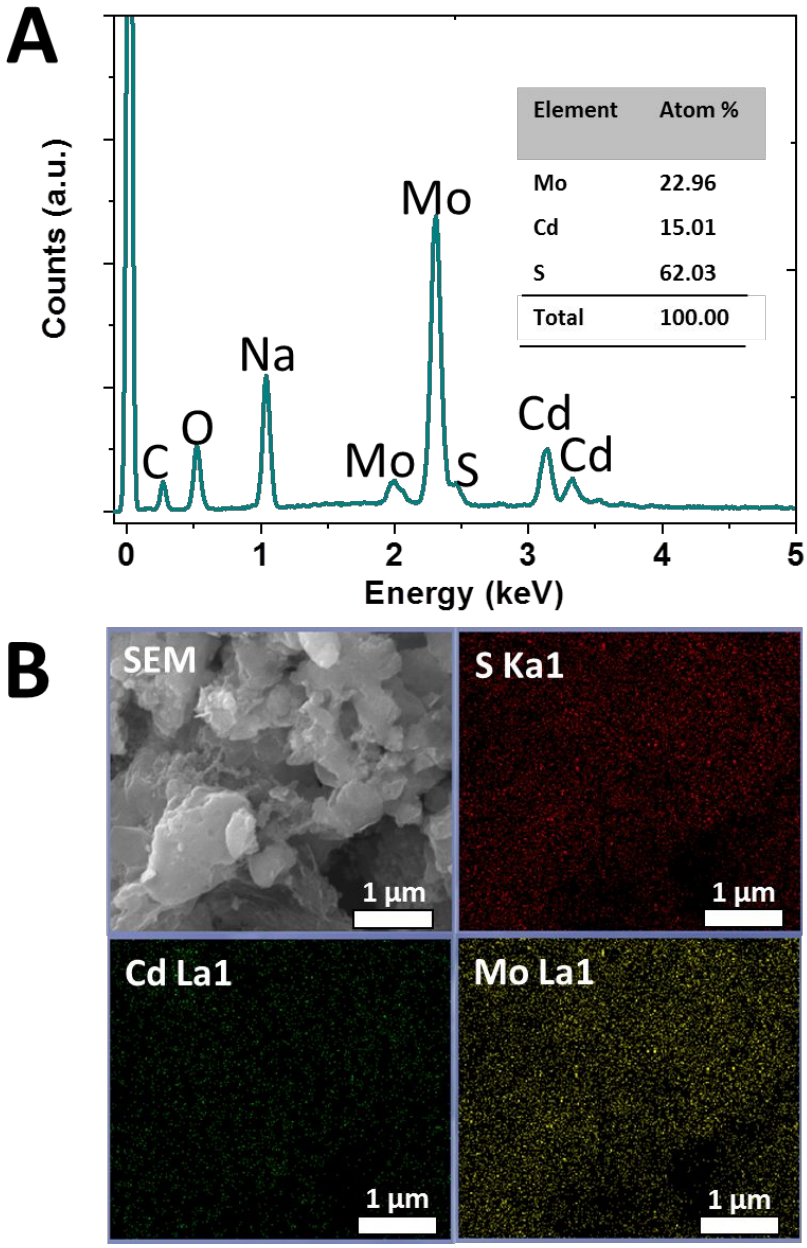

Figure S1. (A) Energy dispersive X-ray (EDS) spectrum and (B) elemental map acquired for few-layered MoS_2/CdS QD heterostructures.

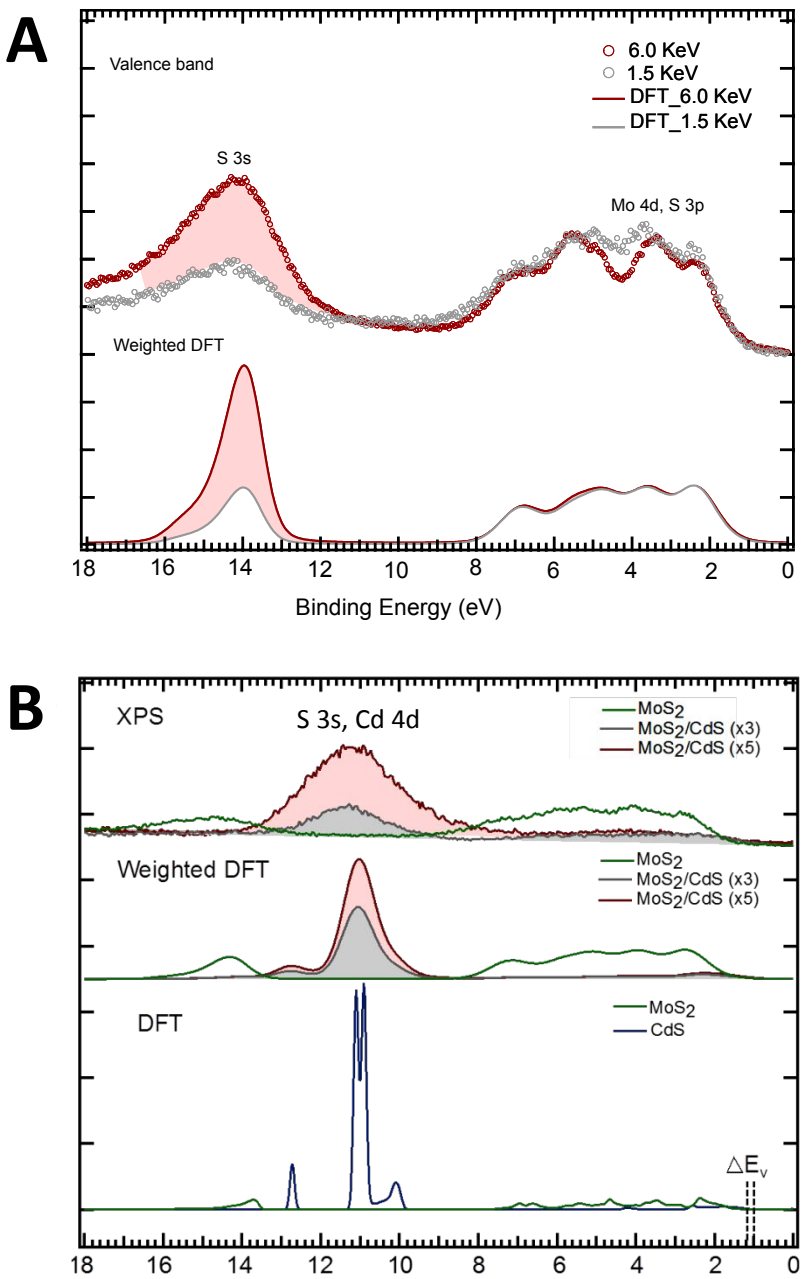

Figure S2. (A) Measured valence band spectra of MoS_2 nanosheets from XPS and HAXPES, compared to weighted spectral simulations of bulk MoS_2 derived from DFT. (B) Valence band spectra from XPS of MoS_2 with MoS_2/CdS (x3), and MoS_2/CdS (x5) heterostructures compared with weighted DFT with a VB offset of 0.2 eV between MoS_2 and CdS, expanded to include the semicore-levels used to assist with the energy alignment.

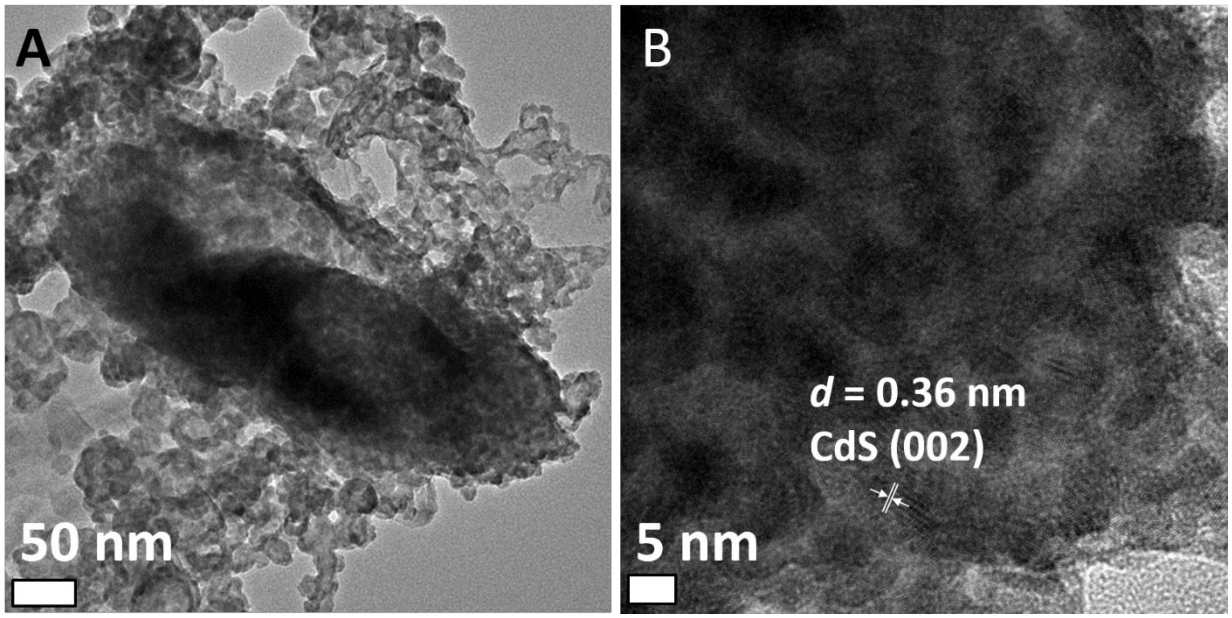

Figure S3. A) Low and B) high-magnification TEM images acquired for MoS_2/CdS heterostructures (×5). At these particle loadings, a substantial population of CdS QDs not directly interfaced with MoS_2 layers are observed.

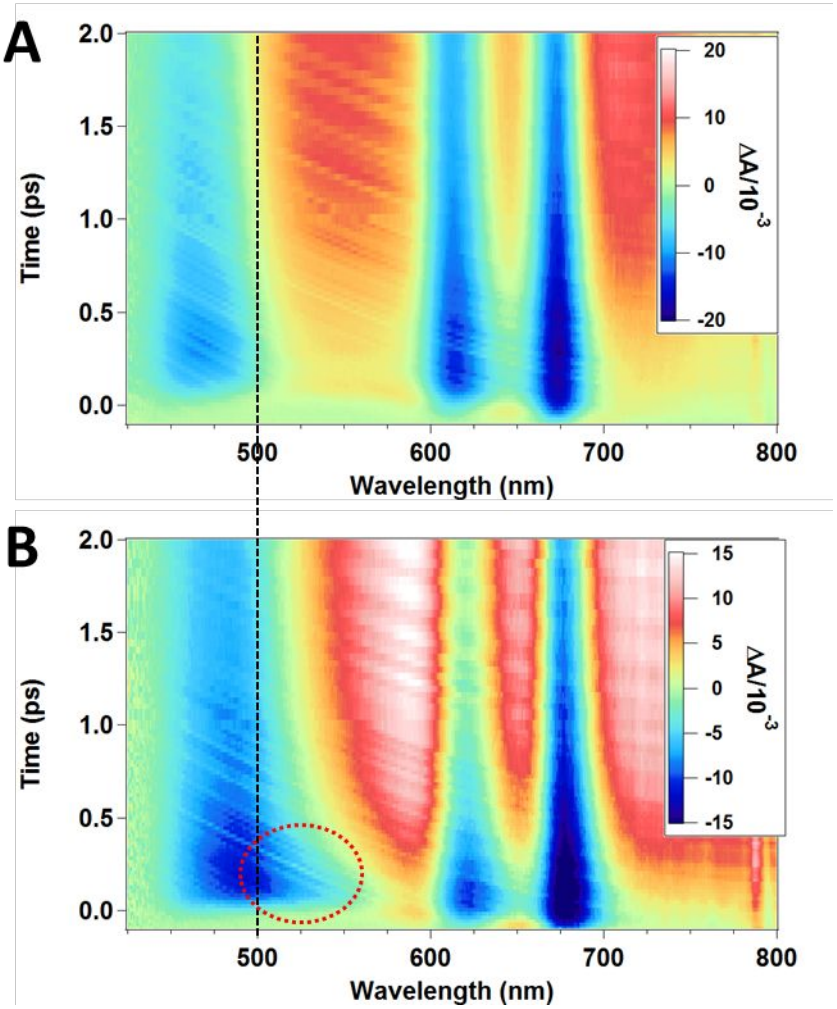

Figure S4. Picosecond TA spectroscopy color map up to 2 ps from initial excitation for A) bare MoS_2 and B) few-layered MoS_2/CdS QD heterostructures upon excitation with a pump wavelength of 360 nm. The dotted red circles delineate the excitonic bleach feature characteristic of CdS QDs, which is lost within 0.5 ps.

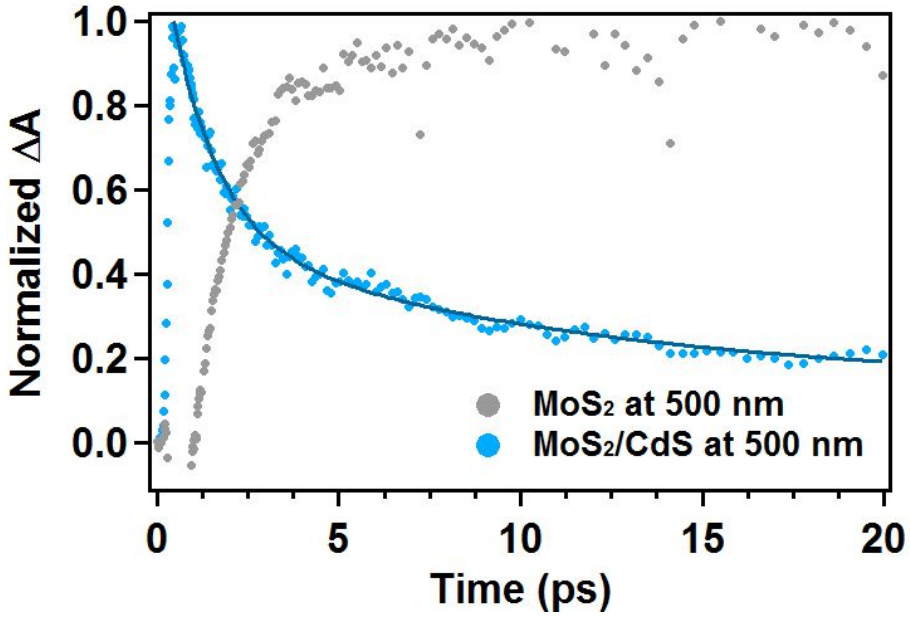

Figure S5. Kinetic decay trace (dotted line) and fitting (solid line) for MoS_2 (grey) and MoS_2/CdS (blue) at a probe wavelength of 500 nm using a monoexponential function for analyzing the electron transfer kinetics from CdS QDs to MoS_2. The fitting parameters are A_0 (0.31±0.01), A (1.00±0.01), and τ (1.8±0.1 ps) yielding a χ^2 of 0.1123.

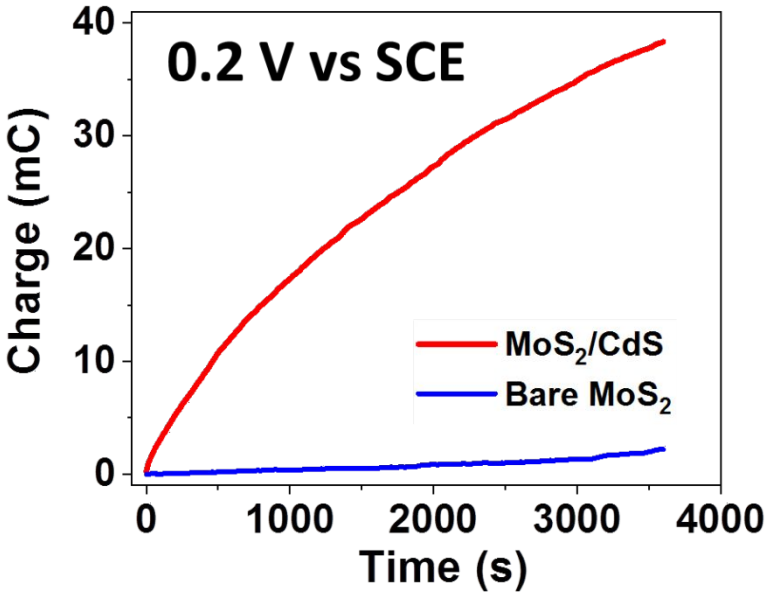

Figure S6. Chronocoulometry data collected at 0.2V *versus* SCE for MoS_2/CdS heterostructures (red) and bare MoS_2 (blue).

Table S1. Kinetic fitting parameters and calculated average lifetimes for nanosecond TA decay traces of bare MoS_2 nanosheets and MoS_2/CdS-QD heterostructures.

Sample	λ_{pump} (nm)	λ_{probe} (nm)	ΔA_0	A_1	τ_1 (ns)	A_2	τ_2 (ns)	A_3	τ_3 (ns)	$<\tau>$ (ns)	χ^2
MoS_2	360	458	0.04 (±0.02)	1.25 (±0.23)	4.18 (±0.73)	0.49 (±0.04)	38.37 (±6.42)	0.13 (±0.03)	334.5 (±166.0)	36.36 (±4.93)	0.164
MoS_2	360	612	0.05 (±0.01)	0.91 (±0.23)	3.11 (±0.56)	0.49 (±0.02)	32.00 (±3.09)	0.33 (±0.02)	183.2 (±15.3)	46.14 (±6.30)	0.036
MoS_2	360	672	0.05 (±0.01)	0.31 (±0.05)	18.38 (±3.15)	0.50 (±0.05)	84.54 (±17.50)	0.23 (±0.07)	383.0 (±144.0)	130.48 (±15.20)	0.028
MoS_2/CdS	360	485	0.11 (±0.01)	1.00 (±0.47)	3.57 (±1.41)	0.29 (±0.06)	30.63 (±12.60)	0.20 (±0.04)	263.2 (±102.0)	43.02 (±14.15)	0.311
MoS_2/CdS	360	615	0.13 (±0.01)	0.94 (±0.19)	3.74 (±0.65)	0.35 (±0.02)	35.92 (±5.19)	0.28 (±0.01)	365.5 (±55.3)	75.59 (±9.44)	0.070
MoS_2/CdS	360	675	0.12 (±0.01)	0.57 (±0.10)	6.86 (±1.68)	0.28 (±0.07)	78.19 (±32.40)	0.26 (±0.04)	638.2 (±585.0)	173.81 (±21.44)	0.247

Table S2. Kinetic fitting parameters and calculated average lifetimes for picosecond TA decay traces of bare MoS_2 nanosheets and MoS_2/CdS-QD heterostructures.

Sample	λ_{pump} (nm)	λ_{probe} (nm)	ΔA_0	A_1	τ_1 (ps)	A_2	τ_2 (ps)	A_3	τ_3 (ps)	$<\tau>$ (ps)	χ^2
MoS_2	360	460	0.179 (±0.007)	0.635 (±0.022)	1.206 (±0.100)	0.193 (±0.022)	7.424 (±2.690)	0.134 (±0.009)	174.8 (±75.0)	26.69 (±1.065)	0.442
MoS_2	360	615	0.413 (±0.044)	0.687 (±0.024)	0.946 (±0.062)	0.052 (±0.013)	13.665 (±7.320)	0.082 (±0.039)	701.34 (±150.1)	71.45 (±4.19)	0.290
MoS_2	360	670	0.334 (±0.044)	0.939 (±0.021)	1.208 (±0.063)	0.050 (±0.023)	10.096 (±6.422)	0.050 (±0.048)	2000.0 (±500.5)	97.82 (±5.40)	0.022
MoS_2/CdS	360	475	0.128 (±0.004)	0.560 (±0.018)	1.676 (±0.109)	0.238 (±0.019)	13.485 (±1.910)	0.171 (±0.009)	242.4 (±26.5)	47.09 (±1.44)	0.228
MoS_2/CdS	360	615	0.338 (±0.007)	0.729 (±0.016)	0.854 (±0.039)	0.095 (±0.013)	8.220 (±1.640)	0.095 (±0.006)	754.5 (±141.0)	79.53 (±1.86)	0.117
MoS_2/CdS	360	670	0.327 (±0.010)	0.689 (±0.013)	1.216 (±0.040)	0.044 (±0.009)	47.074 (±21.600)	0.117 (±0.009)	752.6 (±202.0)	107.16 (±2.58)	0.195